CERN-PH-EP-2012-233
12 Aug 2012

Centrality dependence of charged particle production at large transverse momentum in Pb–Pb collisions at $\sqrt{s_{\text{NN}}} = 2.76$ TeV

ALICE Collaboration*

Abstract

The inclusive transverse momentum (p_T) distributions of primary charged particles are measured in the pseudo-rapidity range $|\eta| < 0.8$ as a function of event centrality in Pb–Pb collisions at $\sqrt{s_{\text{NN}}} = 2.76$ TeV with ALICE at the LHC. The data are presented in the p_T range $0.15 < p_T < 50$ GeV/ c for nine centrality intervals from 70–80% to 0–5%. The results in Pb–Pb are presented in terms of the nuclear modification factor R_{AA} using a pp reference spectrum measured at the same collision energy. We observe that the suppression of high- p_T particles strongly depends on event centrality. The yield is most suppressed in central collisions (0–5%) with $R_{\text{AA}} \approx 0.13$ at $p_T = 6$ –7 GeV/ c . Above $p_T = 7$ GeV/ c , there is a significant rise in the nuclear modification factor, which reaches $R_{\text{AA}} \approx 0.4$ for $p_T > 30$ GeV/ c . In peripheral collisions (70–80%), only moderate suppression ($R_{\text{AA}} = 0.6$ –0.7) and a weak p_T dependence is observed. The measured nuclear modification factors are compared to other measurements and model calculations.

arXiv:1208.2711v3 [hep-ex] 23 Jun 2016

*See Appendix A for the list of collaboration members

1 Introduction

High-energy collisions of heavy-ions enable the study of hot and dense strongly interacting matter [1–5]. At sufficiently high temperature, it is expected that partons (quarks and gluons) are the dominant degrees of freedom. During the very early stage of the collision, some of the incoming partons experience scatterings with large momentum transfers. These partons lose energy when they traverse the hot and dense medium that is formed. One of the major goals of the heavy-ion physics programme at the LHC is to understand the underlying mechanisms for parton energy loss and use this as a tool to probe the properties of the medium.

Parton energy loss in heavy-ion collisions was first observed at RHIC as the suppression of high- p_T particle production in Au–Au collisions compared to expectations from an independent superposition of nucleon-nucleon collisions [6–9]. At RHIC, the particle production in central (0–5%) Au–Au collisions at $\sqrt{s_{NN}} = 200$ GeV is suppressed by a factor of 5 at $p_T = 5–6$ GeV/c [8, 9], and is consistent with being independent of p_T over the measured range $5 < p_T < 20$ GeV/c [10].

The increase of the charged particle density ($dN_{ch}/d\eta$) at mid-rapidity from RHIC energies to actual LHC energies by a factor of around 2.2 [11] implies a similar increase in energy density. However, the observed suppression of high- p_T particle production also depends on the ratio of quarks to gluons due to their different color factors, and on the steepness of the p_T spectra of the scattered partons. At the LHC the initial parton p_T spectra are less steep than at RHIC and the ratio of gluons to quarks at a given p_T is higher [12]. The measurement of high- p_T hadron production at the LHC helps to disentangle the effects which cause the suppression and provides a critical test of existing energy loss calculations [13]. In particular, the large p_T reach provides a means to study the dependence of the energy loss on the initial parton energy.

We present a measurement of the p_T distributions of charged particles in $0.15 < p_T < 50$ GeV/c with pseudo-rapidity $|\eta| < 0.8$, where $\eta = -\ln[\tan(\theta/2)]$, with θ the polar angle between the charged particle direction and the beam axis. Results are presented for different centrality intervals in Pb–Pb collisions at $\sqrt{s_{NN}} = 2.76$ TeV. They are compared with measurements in pp collisions, by calculating the nuclear modification factor

$$R_{AA}(p_T) = \frac{d^2N_{ch}^{AA}/d\eta dp_T}{\langle T_{AA} \rangle d^2\sigma_{ch}^{pp}/d\eta dp_T} \quad (1)$$

where N_{ch}^{AA} and σ_{ch}^{pp} represent the charged particle yield in nucleus-nucleus (AA) collisions and the cross section in pp collisions, respectively. The nuclear overlap function T_{AA} is calculated from the Glauber model [14] and averaged over each centrality interval, $\langle T_{AA} \rangle = \langle N_{coll} \rangle / \sigma_{inel}^{NN}$, where $\langle N_{coll} \rangle$ is the average number of binary nucleon-nucleon collisions and σ_{inel}^{NN} is the inelastic nucleon-nucleon cross section.

Early results from ALICE [15] showed that the production of charged particles in central (0–5%) Pb–Pb collisions at $\sqrt{s_{NN}} = 2.76$ TeV is suppressed by more than a factor of 6 at $p_T = 6–7$ GeV/c compared to an independent superposition of nucleon-nucleon collisions, and that the suppression is stronger than that observed at RHIC. The present data extend the study of high- p_T particle suppression in Pb–Pb out to $p_T = 50$ GeV/c with a systematic study of the centrality dependence.

Moreover, the systematic uncertainties related to the pp reference were significantly reduced with respect to the previous measurement by using the p_T distribution measured in pp collisions at $\sqrt{s} = 2.76$ TeV [16].

Table 1: Average values of the number of participating nucleons $\langle N_{\text{part}} \rangle$ and the nuclear overlap function $\langle T_{\text{AA}} \rangle$ [14] for the centrality intervals used in the analysis.

Centrality	$\langle N_{\text{part}} \rangle$	$\langle T_{\text{AA}} \rangle$ (mb $^{-1}$)
0–5%	383 ± 3	26.4 ± 1.1
5–10%	330 ± 5	20.6 ± 0.9
10–20%	261 ± 4	14.4 ± 0.6
20–30%	186 ± 4	8.7 ± 0.4
30–40%	129 ± 3	5.0 ± 0.2
40–50%	85 ± 3	2.68 ± 0.14
50–60%	53 ± 2	1.32 ± 0.09
60–70%	30.0 ± 1.3	0.59 ± 0.04
70–80%	15.8 ± 0.6	0.24 ± 0.03

2 Experiment and Data Analysis

The ALICE detector is described in [17]. The Inner Tracking System (ITS) and the Time Projection Chamber (TPC) are used for vertex finding and tracking. The minimum-bias interaction trigger was derived from signals from the forward scintillators (VZERO), and the two innermost layers of the ITS (Silicon Pixel Detector - SPD). The collision centrality is determined using the VZERO. In addition, the information from two neutron Zero Degree Calorimeters (ZDCs) positioned at ± 114 m from the interaction point was used to remove contributions from beam-gas and electromagnetic interactions. The trigger and centrality selection are described in more detail in [11].

The following analysis is based on $1.6 \cdot 10^7$ minimum-bias Pb–Pb events recorded by ALICE in 2010. For this study, the events are divided into nine centrality intervals from the 70–80% to the 0–5% most central Pb–Pb collisions, expressed in percentage of the total hadronic cross section. The event centrality can be related to the number of participating nucleons N_{part} and the nuclear overlap function T_{AA} by using simulations based on the Glauber model [14]. The average values of N_{part} and T_{AA} for each centrality interval, $\langle N_{\text{part}} \rangle$ and $\langle T_{\text{AA}} \rangle$, along with their corresponding systematic uncertainties, are listed in Table 1. The errors include the experimental uncertainties on the inelastic nucleon-nucleon cross section $\sigma_{\text{inel}}^{\text{NN}} = 64 \pm 5$ mb at $\sqrt{s_{\text{NN}}} = 2.76$ TeV [18] and on the parameters of the nuclear density profile used in the Glauber simulations (more details in [11]).

The primary vertex position was determined from the tracks reconstructed in the ITS and the TPC by using an analytic χ^2 minimization method, applied after approximating each of the tracks by a straight line in the vicinity of their common origin. The event is accepted if the coordinate of the reconstructed vertex measured along the beam direction (z -axis) is within ± 10 cm around the nominal interaction point. The event vertex reconstruction is fully efficient for the event centralities covered.

Primary charged particles are defined as all prompt particles produced in the collision, including decay products, except those from weak decays of strange hadrons. A set of standard cuts based on the number of space points and the quality of the momentum fit in the TPC and ITS is applied to the reconstructed tracks. Track candidates in the TPC are required to have hits in at least 120 (out of a maximum of 159) pad-rows and χ^2 per point of the momentum fit smaller than 4. Such tracks are projected to the ITS and used for further analysis if at least 2 matching hits (out of a maximum of 6) in the ITS, including at least one in the SPD, are found. In addition, the χ^2 per point of the momentum fit in the ITS must be smaller than 36. In order to improve the purity of primary track reconstruction at high p_{T} we developed a procedure where we compare tracking information from the combined ITS and TPC track reconstruction algorithm to that derived only from the TPC and constrained by the interaction vertex point. We calculated the $\chi_{\text{TPC-ITS}}^2$ between these tracks using the following formula

Table 2: Contribution to the systematic uncertainties on the p_T spectra (0.15–50 GeV/c) for the most central and peripheral Pb–Pb collisions. Also listed are the systematic uncertainties on the pp reference (0.15–50 GeV/c) [16].

Centrality class	0–5%	70–80%
Centrality selection	0.4%	6.7%
Event selection	3.2%	3.4%
Track selection	4.1–7.3%	3.6–6.0%
Tracking efficiency	5%	5%
p_T resolution correction	<1.8%	<3%
Material budget	0.9–1.2%	0.5–1.7%
Particle composition	0.6–10%	0.5–7.7%
MC generator	2.5%	1.5%
Secondary particle rejection	<1%	<1%
Total for p_T spectra	8.2–13.5%	10.3–13.4%
Total for pp reference	6.3–18.8%	
pp reference normalization	1.9%	

$$\chi_{\text{TPC-ITS}}^2 = (\mathbf{v}_{\text{TPC}} - \mathbf{v}_{\text{TPC-ITS}})^T \cdot (\mathbf{C}_{\text{TPC}} + \mathbf{C}_{\text{TPC-ITS}})^{-1} \cdot (\mathbf{v}_{\text{TPC}} - \mathbf{v}_{\text{TPC-ITS}}) \quad (2)$$

where \mathbf{v}_{TPC} , $\mathbf{v}_{\text{TPC-ITS}}$ and \mathbf{C}_{TPC} , $\mathbf{C}_{\text{TPC-ITS}}$ represent the measured track parameter vectors $\mathbf{v} = (x, y, z, \theta, \phi, 1/p_T)$ and their covariance matrices, respectively. If the $\chi_{\text{TPC-ITS}}^2$ is larger than 36 the track candidate is rejected. At $p_T = 0.15\text{--}50$ GeV/c, this procedure removes about 2–7% (1–3%) of the reconstructed tracks in the most central (peripheral) collisions. This procedure in fact removes high- p_T fake tracks, which originate from spurious matches of low p_T particles in the TPC to hits in the ITS, and would result in an incorrect momentum assignment.

Finally, tracks are rejected from the sample if their distance of closest approach to the reconstructed vertex in the longitudinal direction d_z is larger than 2 cm or $d_{xy} > 0.018\text{ cm} + 0.035\text{ cm} \cdot p_T^{-1}$ in the transverse direction with p_T in GeV/c, which corresponds to 7 standard deviations of the resolution in d_{xy} (see [19] for details). The upper limit on the d_z ($d_z < 2$ cm) was set to minimize the contribution of tracks coming from pileup and beam-gas background events. These cuts reject less than 0.5% of the reconstructed tracks independently of p_T and collision centrality.

The efficiency and purity of the primary charged particle selection are estimated using a Monte Carlo simulation with HIJING [20] events and a GEANT3 [21] model of the detector response. We used a HIJING tune which reproduces approximately the measured charged particle density in central collisions [11]. In the most central events, the overall primary charged particle reconstruction efficiency (tracking efficiency and acceptance) in $|\eta| < 0.8$ is 36% at $p_T = 0.15$ GeV/c and increases to 65% for $p_T > 0.6$ GeV/c. In the most peripheral events the efficiency is larger than that for the central events by about 1–3%. The contribution from secondary particles was estimated using the d_{xy} distributions of data and HIJING and is consistent with the measured strangeness to charged particle ratio from the reconstruction of K_s^0 , Λ and $\bar{\Lambda}$ invariant mass peaks in Pb–Pb [22]. The total contribution from secondary tracks at $p_T = 0.15$ GeV/c is 13 (7)% for central (peripheral) events and decreases to about 0.6% above $p_T = 4$ GeV/c for both central and peripheral events. From a systematic variation of the $\chi_{\text{TPC-ITS}}^2$ cut and comparison of track properties in MC to data we conclude that the number of properly reconstructed tracks rejected as high- p_T fake tracks is around 1–2% (0.5–1%) in the most central (peripheral) collisions. We also conclude that the contribution from the high- p_T fake tracks to the p_T spectra is negligible independently of the collision centrality and p_T .

The transverse momentum of charged particles is reconstructed from the track curvature measured in the magnetic field $B = 0.5$ T using the ITS and TPC detectors. The p_T resolution is estimated from the track

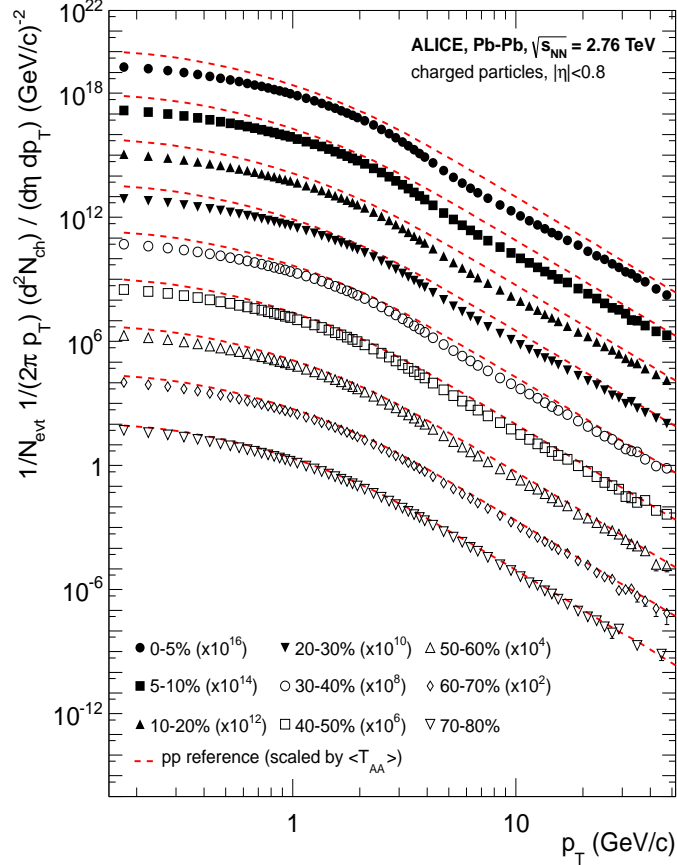


Fig. 1: Charged particle p_T distribution measured in Pb–Pb collisions in different centrality intervals. The spectra are scaled for better visibility. The dashed lines show the pp reference [16] spectra scaled by the nuclear overlap function determined for each centrality interval (Table 1) and by the Pb–Pb spectra scaling factors. The systematic and statistical uncertainties for Pb–Pb are added quadratically. The uncertainties on the pp reference are not shown.

residuals to the momentum fit and verified by cosmic muon events, and the width of the invariant mass peaks of Λ , $\bar{\Lambda}$ and K_s^0 reconstructed from their decays to two charged particles. For the selected tracks the relative p_T resolution ($\sigma(p_T)/p_T$) amounts to 3.5% at $p_T = 0.15$ GeV/ c , has a minimum of 1% at $p_T = 1$ GeV/ c , and increases linearly to 10% at $p_T = 50$ GeV/ c . It is independent of the centrality of the selected events. From the study of the invariant mass distributions of Λ and K_s^0 as a function of p_T we estimate that the relative uncertainty on the p_T resolution is around 20%. From the mass difference between Λ and $\bar{\Lambda}$ and the ratio of positively to negatively charged tracks, assuming charge symmetry at high p_T , the upper limit of the systematic uncertainty of the momentum scale is estimated to be $|\Delta(p_T)/p_T| < 0.005$ at $p_T = 50$ GeV/ c . This has an effect of around 1.5% on the yield of the measured spectra at the highest p_T . To account for the finite p_T resolution, correction factors for the reconstructed p_T spectra at $p_T > 10$ GeV/ c are derived using a folding procedure. The corrections depend on collision centrality due to the change of the spectral shape and reach 4 (8)% at $p_T = 50$ GeV/ c in the most central (peripheral) collisions.

The systematic uncertainties on the p_T spectra are summarized in Table 2. The systematic uncertainties related to centrality selection were estimated by a comparison of the p_T spectra when the limits of the centrality classes are shifted by $\pm 1\%$ (e.g. for the 70–80% centrality class, 70.7–80.8% and 69.3–79.2%), which is a relative uncertainty on the fraction of the hadronic cross section used in the Glauber fit [11] to determine the centrality classes. We also varied the event and track quality selection criteria and the Monte Carlo assumptions to estimate systematic uncertainties on the p_T spectra. In particular,

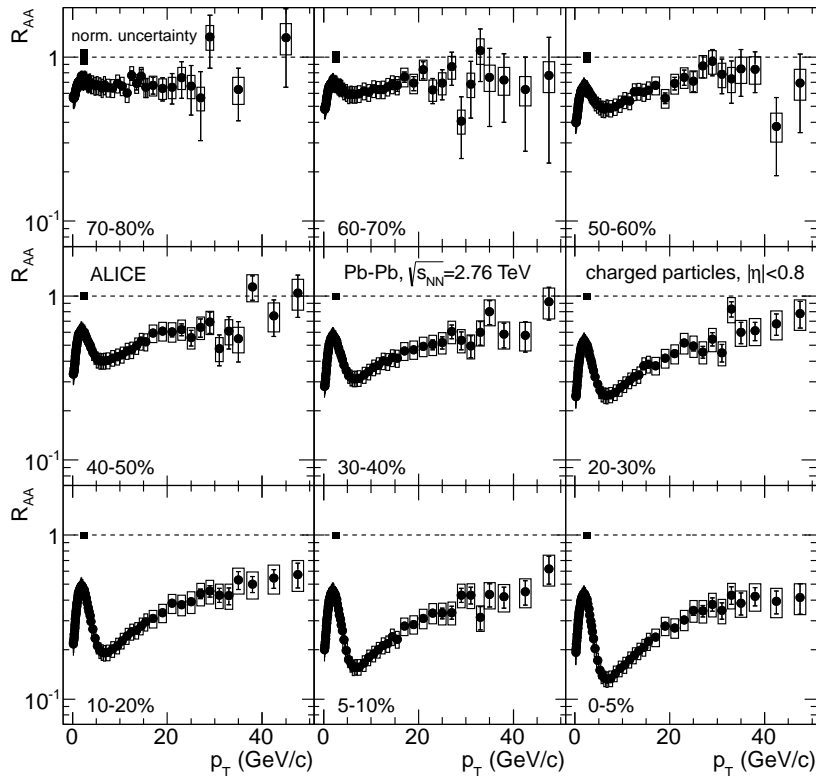


Fig. 2: Nuclear modification factor R_{AA} of charged particles measured in Pb–Pb collisions in nine centrality intervals. The boxes around data points denote p_T -dependent systematic uncertainties. The systematic uncertainties on the normalization which are related to $\langle T_{AA} \rangle$ and the normalization of the pp data are added in quadrature and shown as boxes at $R_{AA} = 1$.

we studied a variation of the most abundant charged particle species (pions, kaons, protons) by $\pm 30\%$ to match the measured ratios and their uncertainties [22]. The material budget was varied by $\pm 7\%$ [23], and the secondary yield from strangeness decays in the Monte Carlo by $\pm 30\%$ to match the measured d_{xy} distributions. Moreover, we used a different event generator, DPMJET [24], to calculate MC correction maps. The systematic uncertainties on the p_T spectra, related to the high- p_T fake track rejection procedure, were estimated by varying the track matching criteria in the range $25 < \chi^2_{\text{TPC-ITS}} < 49$, and amount to 1–4% (1–2%) in the most central (peripheral) collisions. The total systematic uncertainties on the corrected p_T spectra depend on p_T and event centrality and amount to 8.2–13.5% (10.3–13.4%) in the most central (peripheral) collisions.

A dedicated run of the LHC to collect pp reference data at $\sqrt{s} = 2.76$ TeV took place in March 2011. Data taken in this run were used to measure the charged particle p_T spectrum that forms the basis of the pp reference spectrum for R_{AA} . Using these data the systematic uncertainties in R_{AA} related to the pp reference could be significantly improved (Table 2) compared to the previous publication [15], allowing for an exploration of high- p_T particle suppression in Pb–Pb out to 50 GeV/c. More details about the pp reference determination can be found in [16].

3 Results

The fully corrected p_T spectra of inclusive charged particles measured in Pb–Pb collisions at $\sqrt{s_{NN}} = 2.76$ TeV in nine different centrality intervals, and the scaled pp reference spectra are shown in Fig. 1.

At low p_T , the transverse momentum spectra differ from the pp reference. This is in agreement with the previously observed scaling behavior of the total charged particle production as a function of centrality [11]. A marked depletion of the spectra at high transverse momentum ($p_T > 5$ GeV/c) develops gradually as centrality increases, indicating strong suppression of high- p_T particle production in central collisions.

The nuclear modification factors for nine centrality intervals are shown in Fig. 2. In peripheral collisions (70–80%), only moderate suppression ($R_{AA} = 0.6$ – 0.7) and a weak p_T dependence is observed. Towards more central collisions, a pronounced minimum at about $p_T = 6$ – 7 GeV/c develops while for $p_T > 7$ GeV/c there is a significant rise of the nuclear modification factor. This rise becomes gradually less steep with increasing p_T . In the most central collisions (0–5%), the yield is most suppressed, $R_{AA} \approx 0.13$ at $p_T = 6$ – 7 GeV/c, and R_{AA} reaches ≈ 0.4 with no significant p_T dependence for $p_T > 30$ GeV/c.

The dependence of R_{AA} on the collision centrality, expressed in terms of N_{part} and the charged particle multiplicity density ($dN_{\text{ch}}/d\eta$), are shown in Fig. 3 for different intervals of p_T . Also shown are results from PHENIX at RHIC in Au–Au collisions at $\sqrt{s_{\text{NN}}} = 200$ GeV [9]. The strongest centrality dependence is observed for particles with $5 < p_T < 7$ GeV/c. At higher p_T , the centrality dependence weakens gradually. In comparison to results from RHIC, the LHC data in the same p_T window show a suppression which is larger by a factor of about 1.2 at all $\langle N_{\text{part}} \rangle$ (Fig. 3, top panel). This implies that the shape of the N_{part} dependence at RHIC and the LHC is very similar when the same p_T is compared, indicating a strong relation between collision geometry and energy loss. The overall increase of suppression at the LHC as compared to RHIC may be expected from the larger density and longer lifetime of the fireball. The suppression reaches similar values when results from RHIC are compared to results from the LHC in terms of $dN_{\text{ch}}/d\eta$, as shown in Fig. 3 (bottom panel). Larger values of suppression than at RHIC are observed in central collisions at the LHC, where the charged particle multiplicity exceeds that of the most central collisions at RHIC. It should be noted that the suppression at a given centrality results from a subtle interplay between the parton p_T spectrum, the quark-to-gluon ratio, and the medium density, all of which exhibit a significant energy dependence. Further model studies are needed to evaluate their relative contributions.

The ALICE measurement of R_{AA} in the most central Pb–Pb collisions (0–5%) is compared to the CMS result [25] in Fig. 4. Both measurements agree within their respective statistical and systematic uncertainties.

In Fig. 4, the measured R_{AA} for 0–5% central collisions is also compared to model calculations. All selected models use RHIC data to calibrate the medium density and were available before the preliminary version of the data reported in this paper. All model calculations except WHDG [26] use a hydrodynamical description of the medium, but different extrapolation assumptions from RHIC to LHC. A variety of energy loss formalisms is used. An increase of R_{AA} due to a decrease of the relative energy loss with increasing p_T is seen for all the models.

The curves labeled WHDG, ASW, and Higher Twist (HT) are based on analytical radiative energy loss formulations that include interference effects. Of those curves, the multiple soft gluon approximation (ASW [27]) and the opacity expansion (WHDG [26]) show a larger suppression than seen in the measurement, while one of the HT curves (Chen [28]) with lower density provides a good description. The other HT (Majumder [29]) curve shows a stronger rise with p_T than measured. The elastic energy loss model by Renk (elastic) [30] does not rise steeply enough with p_T and overshoots the data at low p_T . The YaJEM-D model [31], which is based on medium-induced virtuality increases in a parton shower, shows too strong a p_T -dependence of R_{AA} due to a formation time cut-off.

A more systematic study of the energy loss formalisms, preferably with the same model(s) for the medium density is needed to rule out or confirm the various effects. Deviations of the nuclear parton distribution functions (PDFs) from a simple scaling of the nucleon PDF with mass number A (e.g. shad-

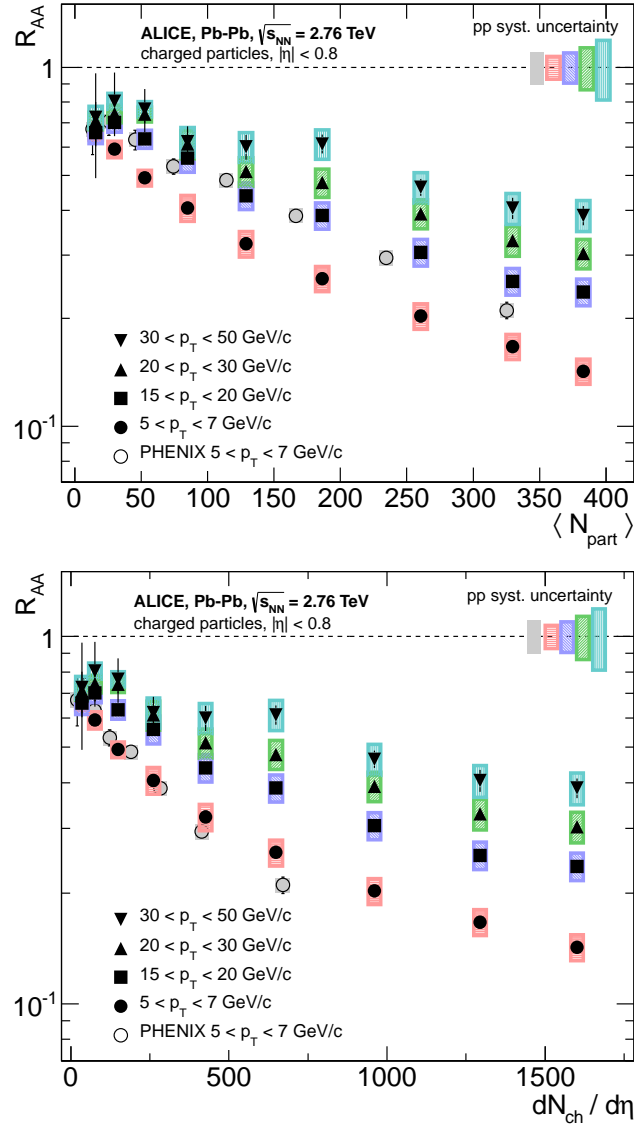


Fig. 3: Nuclear modification factor R_{AA} of charged particles as a function of $\langle N_{part} \rangle$ (top panel) and $dN_{ch}/d\eta$ (bottom panel) measured by ALICE in Pb–Pb collisions in different p_T -intervals, compared to PHENIX results in $5 < p_T < 7$ GeV/c [9]. The boxes around the data represent the p_T -dependent uncertainties on the Pb–Pb p_T spectra. The boxes at $R_{AA} = 1$ represent the systematic uncertainties on the pp reference in different p_T -intervals (p_T -interval increases from left to right, the left-most is for PHENIX). The systematic uncertainties on the overall normalization for ALICE and PHENIX are not shown.

owing) are also expected to affect the nuclear modification factor. These effects are predicted to be small for $p_T > 10$ GeV/c at the LHC [26] and will be quantified in future p–Pb measurements.

4 Summary

We have reported the measurements of charged particle p_T spectra and nuclear modification factors R_{AA} as a function of event centrality in Pb–Pb collisions at $\sqrt{s_{NN}} = 2.76$ TeV. The results indicate a strong suppression of charged particle production in Pb–Pb collisions and a characteristic centrality and p_T dependence of the nuclear modification factors. In central collisions (0–5%) the yield is most strongly suppressed ($R_{AA} \approx 0.13$) at $p_T = 6$ –7 GeV/c. Above $p_T = 7$ GeV/c, there is a significant rise in the

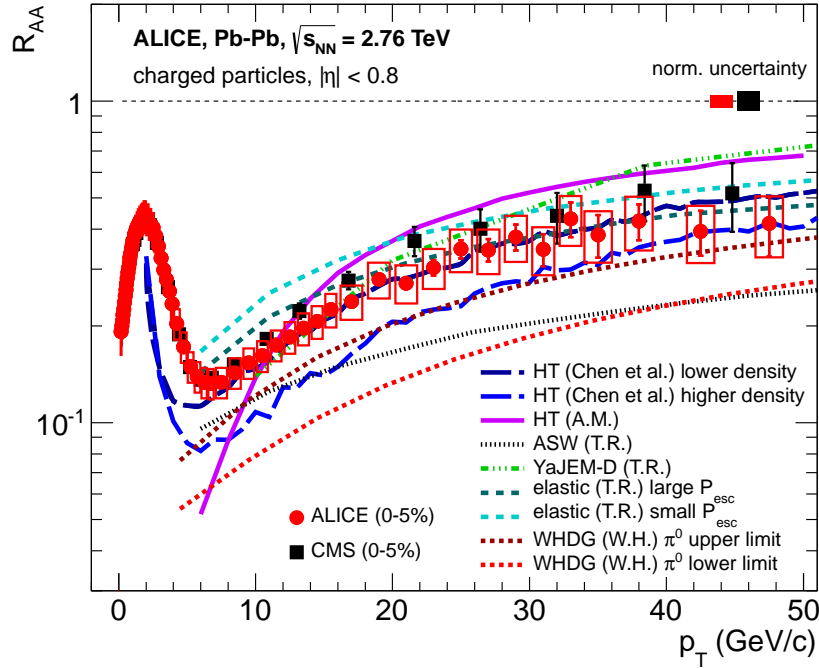


Fig. 4: Nuclear modification factor R_{AA} of charged particles measured by ALICE in the most central Pb–Pb collisions (0–5%) in comparison to results from CMS [25] and model calculations [26–31]. The boxes around the data denote p_T -dependent systematic uncertainties. For CMS statistical and systematic uncertainties on R_{AA} are added in quadrature. The systematic uncertainties on the normalization which are related to $\langle T_{AA} \rangle$ and the normalization of the pp data are added in quadrature and shown as boxes at $R_{AA} = 1$ (the right-most is for CMS).

nuclear modification factor, which reaches $R_{AA} \approx 0.4$ for $p_T > 30$ GeV/c. This result is in agreement with the CMS measurement within statistical and systematic uncertainties. The suppression is weaker in peripheral collisions (70–80%) with $R_{AA} = 0.6$ –0.7 and no strong p_T dependence. The observed suppression of high- p_T particles in central Pb–Pb collisions provides evidence for strong parton energy loss and a large medium density at the LHC. We observe that the suppression of charged particles with $5 < p_T < 7$ GeV/c reaches similar values when results from RHIC are compared to results from LHC in terms of the $dN_{ch}/d\eta$. The measured R_{AA} in 0–5% central collisions is compared to model calculations. An increase of R_{AA} due to a decrease of the relative energy loss with increasing p_T is seen for all the models. The measurement presented here, together with measurements of particle correlations [32] and measurements using jet reconstruction [33], will help in understanding the mechanism of jet quenching and the properties of the medium produced in heavy-ion collisions.

5 Acknowledgements

The ALICE collaboration would like to thank all its engineers and technicians for their invaluable contributions to the construction of the experiment and the CERN accelerator teams for the outstanding performance of the LHC complex.

The ALICE collaboration acknowledges the following funding agencies for their support in building and running the ALICE detector:

Calouste Gulbenkian Foundation from Lisbon and Swiss Fonds Kidagan, Armenia;

Conselho Nacional de Desenvolvimento Científico e Tecnológico (CNPq), Financiadora de Estudos e Projetos (FINEP), Fundação de Amparo à Pesquisa do Estado de São Paulo (FAPESP);

National Natural Science Foundation of China (NSFC), the Chinese Ministry of Education (CMOE) and

the Ministry of Science and Technology of China (MSTC);
 Ministry of Education and Youth of the Czech Republic;
 Danish Natural Science Research Council, the Carlsberg Foundation and the Danish National Research Foundation;
 The European Research Council under the European Community's Seventh Framework Programme;
 Helsinki Institute of Physics and the Academy of Finland;
 French CNRS-IN2P3, the 'Region Pays de Loire', 'Region Alsace', 'Region Auvergne' and CEA, France;
 German BMBF and the Helmholtz Association;
 General Secretariat for Research and Technology, Ministry of Development, Greece;
 Hungarian OTKA and National Office for Research and Technology (NKTH);
 Department of Atomic Energy and Department of Science and Technology of the Government of India;
 Istituto Nazionale di Fisica Nucleare (INFN) of Italy;
 MEXT Grant-in-Aid for Specially Promoted Research, Japan;
 Joint Institute for Nuclear Research, Dubna;
 National Research Foundation of Korea (NRF);
 CONACYT, DGAPA, México, ALFA-EC and the HELEN Program (High-Energy physics Latin-American-European Network);
 Stichting voor Fundamenteel Onderzoek der Materie (FOM) and the Nederlandse Organisatie voor Wetenschappelijk Onderzoek (NWO), Netherlands;
 Research Council of Norway (NFR);
 Polish Ministry of Science and Higher Education;
 National Authority for Scientific Research - NASR (Autoritatea Națională pentru Cercetare Științifică - ANCS);
 Federal Agency of Science of the Ministry of Education and Science of Russian Federation, International Science and Technology Center, Russian Academy of Sciences, Russian Federal Agency of Atomic Energy, Russian Federal Agency for Science and Innovations and CERN-INTAS;
 Ministry of Education of Slovakia;
 Department of Science and Technology, South Africa;
 CIEMAT, EELA, Ministerio de Educación y Ciencia of Spain, Xunta de Galicia (Consellería de Educación), CEADEN, Cubaenergía, Cuba, and IAEA (International Atomic Energy Agency);
 Swedish Research Council (VR) and Knut & Alice Wallenberg Foundation (KAW);
 Ukraine Ministry of Education and Science;
 United Kingdom Science and Technology Facilities Council (STFC);
 The United States Department of Energy, the United States National Science Foundation, the State of Texas, and the State of Ohio.

References

- [1] I. Arsene et al. (BRAHMS Collaboration), Nucl. Phys. **A 757** (2005) 1.
- [2] B. B. Back et al. (PHOBOS Collaboration), Nucl. Phys. **A 757** (2005) 28.
- [3] J. Adams et al. (STAR Collaboration), Nucl. Phys. **A 757** (2005) 102.
- [4] K. Adcox et al. (PHENIX Collaboration), Nucl. Phys. **A 757** (2005) 184.
- [5] D. d'Enterria, Phys. Lett. B **596** (2004) 32.
- [6] K. Adcox et al. (PHENIX Collaboration), Phys. Rev. Lett. **88** (2001) 022301.
- [7] C. Adler et al. (STAR Collaboration), Phys. Rev. Lett. **89** (2002) 202301.
- [8] J. Adams et al. (STAR Collaboration), Phys. Rev. Lett. **91** (2003) 172302.
- [9] S. S. Adler et al. (PHENIX Collaboration), Phys. Rev. C **69** (2004) 034910.
- [10] A. Adare et al. (PHENIX Collaboration), Phys. Rev. Lett. **101** (2008) 232301.

- [11] K. Aamodt et al. (ALICE Collaboration), Phys. Rev. Lett. **105** (2010) 252301; Phys. Rev. Lett. **106** (2011) 032301; B. Abelev et al. (ALICE Collaboration), to be published.
- [12] K. J. Eskola, H. Honkanen, C. A. Salgado and U. A. Wiedemann, Nucl. Phys. A **747** (2005) 511.
- [13] N. Armesto et al., arXiv:1106.1106v1 [hep-ph].
- [14] M. Miller, K. Reygers, S. Sanders and P. Steinberg, Annu. Rev. Nucl. Part. Sci. **57** (2007) 205.
- [15] K. Aamodt et al. (ALICE Collaboration), Phys. Lett. B **696** (2011) 30.
- [16] K. Aamodt et al. (ALICE Collaboration), to be published.
- [17] K. Aamodt et al. (ALICE Collaboration), JINST **3** (2008) S08002.
- [18] K. Nakamura et al. (Particle Data Group), J. Phys. G **37** (2010) 075021.
- [19] B. Abelev et al. (ALICE Collaboration), JHEP **1201** (2012) 128.
- [20] X.-N. Wang and M. Gyulassy, Phys. Rev. D **44** (1991) 3501; W.-T. Deng, X.-N. Wang and R. Xu, Phys. Rev. C **83** (2011) 014915.
- [21] R. Brun et al., CERN Program Library Long Write-up, W5013, GEANT Detector Description and Simulation Tool (1994).
- [22] M. Floris et al. (ALICE Collaboration) J. Phys. G: Nucl. Part. Phys. **38** (2011) 124025.
- [23] K. Koch et al. (ALICE Collaboration), Nucl. Phys. A **855** (2011) 281.
- [24] S. Roesler, R. Engel and J. Ranft, arXiv:hep-ph/0012252.
- [25] S. Chatrchyan et al. (CMS Collaboration), Eur. Phys. J. C **72** (2012) 1945.
- [26] W. A. Horowitz and M. Gyulassy, Nucl. Phys. A **872** (2011) 265.
- [27] C. A. Salgado and U. A. Wiedemann, Phys. Rev. D **68** (2003) 014008.
- [28] X.-F. Chen, T. Hirano, E. Wang, X.-N. Wang and H. Zang, Phys. Rev. C **84** (2011) 034902.
- [29] A. Majumder and B. Muller, Phys. Rev. Lett. **105** (2010) 252002.
- [30] T. Renk, H. Holopainen, R. Paatelainen and K. J. Eskola, Phys. Rev. C. **84** (2011) 014906.
- [31] T. Renk, Phys. Rev. C **83** (2011) 024908.
- [32] K. Aamodt et al. (ALICE Collaboration), Phys. Rev. Lett. **108** (2012) 092301.
- [33] B. Abelev et al. (ALICE Collaboration), JHEP **03** (2012) 053.

A The ALICE Collaboration

B. Abelev⁶⁸, J. Adam³⁴, D. Adamová⁷³, A.M. Adare¹²⁰, M.M. Aggarwal⁷⁷, G. Aglieri Rinella³⁰, A.G. Agocs⁶⁰, A. Agostinelli¹⁹, S. Aguilar Salazar⁵⁶, Z. Ahammed¹¹⁶, N. Ahmad¹⁴, A. Ahmad Masoodi¹⁴, S.A. Ahn⁶², S.U. Ahn³⁷, A. Akindinov⁴⁶, D. Aleksandrov⁸⁸, B. Alessandro⁹⁴, R. Alfaro Molina⁵⁶, A. Alici^{97,10}, A. Alkin², E. Almaráz Aviña⁵⁶, J. Alme³², T. Alt³⁶, V. Altini²⁸, S. Altinpinar¹⁵, I. Altsybeev¹¹⁷, C. Andrei⁷⁰, A. Andronic⁸⁵, V. Anguelov⁸², J. Anielski⁵⁴, C. Anson¹⁶, T. Antičić⁸⁶, F. Antinori⁹³, P. Antonioli⁹⁷, L. Aphecetche¹⁰², H. Appelshäuser⁵², N. Arbor⁶⁴, S. Arcelli¹⁹, A. Arend⁵², N. Armesto¹³, R. Arnaldi⁹⁴, T. Aronsson¹²⁰, I.C. Arsene⁸⁵, M. Arslanok⁵², A. Asryan¹¹⁷, A. Augustinus³⁰, R. Averbeck⁸⁵, T.C. Awes⁷⁴, J. Äystö³⁸, M.D. Azmi^{14,79}, M. Bach³⁶, A. Badalá⁹⁹, Y.W. Baek^{63,37}, R. Bailhache⁵², R. Bala⁹⁴, R. Baldini Ferroli¹⁰, A. Baldisseri¹², A. Baldit⁶³, F. Baltasar Dos Santos Pedrosa³⁰, J. Bán⁴⁷, R.C. Baral⁴⁸, R. Barbera²⁵, F. Barile²⁸, G.G. Barnaföldi⁶⁰, L.S. Barnby⁹⁰, V. Barret⁶³, J. Bartke¹⁰⁴, M. Basile¹⁹, N. Bastid⁶³, S. Basu¹¹⁶, B. Bathen⁵⁴, G. Batigne¹⁰², B. Batyunya⁵⁹, C. Baumann⁵², I.G. Bearden⁷¹, H. Beck⁵², N.K. Behera⁴⁰, I. Belikov⁵⁸, F. Bellini¹⁹, R. Bellwied¹¹⁰, E. Belmont-Moreno⁵⁶, G. Bencedi⁶⁰, S. Beole²³, I. Berceau⁷⁰, A. Bercuci⁷⁰, Y. Berdnikov⁷⁵, D. Berenyi⁶⁰, A.A.E. Bergognon¹⁰², D. Berzano⁹⁴, L. Betev³⁰, A. Bhasin⁸⁰, A.K. Bhati⁷⁷, J. Bhom¹¹⁴, L. Bianchi²³, N. Bianchi⁶⁵, C. Bianchin²⁰, J. Bielčik³⁴, J. Bielčiková⁷³, A. Bilandzic⁷¹, S. Bjelogrić⁴⁵, F. Blanco⁸, F. Blanco¹¹⁰, D. Blau⁸⁸, C. Blume⁵², M. Boccioli³⁰, N. Bock¹⁶, S. Böttger⁵¹, A. Bogdanov⁶⁹, H. Bøggild⁷¹, M. Bogolyubsky⁴³, L. Boldizsár⁶⁰, M. Bombara³⁵, J. Book⁵², H. Borel¹², A. Borissov¹¹⁹, S. Bose⁸⁹, F. Bossú^{79,23}, M. Botje⁷², E. Botta²³, B. Boyer⁴², E. Braidot⁶⁷, P. Braun-Munzinger⁸⁵, M. Bregant¹⁰², T. Breitner⁵¹, T.A. Browning⁸³, M. Broz³³, R. Brun³⁰, E. Bruna^{23,94}, G.E. Bruno²⁸, D. Budnikov⁸⁷, H. Buesching⁵², S. Bufalino^{23,94}, O. Busch⁸², Z. Buthelezi⁷⁹, D. Caballero Orduna¹²⁰, D. Caffarri^{20,93}, X. Cai⁵, H. Caines¹²⁰, E. Calvo Villar⁹¹, P. Camerini²¹, V. Canoa Roman⁹, G. Cara Romeo⁹⁷, F. Carena³⁰, W. Carena³⁰, N. Carlin Filho¹⁰⁷, F. Carminati³⁰, A. Casanova Díaz⁶⁵, J. Castillo Castellanos¹², J.F. Castillo Hernandez⁸⁵, E.A.R. Casula²², V. Catanescu⁷⁰, C. Cavicchioli³⁰, C. Ceballos Sanchez⁷, J. Cepila³⁴, P. Cerello⁹⁴, B. Chang^{38,123}, S. Chapeland³⁰, J.L. Charvet¹², S. Chattopadhyay¹¹⁶, S. Chattopadhyay⁸⁹, I. Chawla⁷⁷, M. Cherney⁷⁶, C. Cheshkov^{30,109}, B. Cheynis¹⁰⁹, V. Chibante Barroso³⁰, D.D. Chinellato¹⁰⁸, P. Chochula³⁰, M. Chojnacki⁴⁵, S. Choudhury¹¹⁶, P. Christakoglou⁷², C.H. Christensen⁷¹, P. Christiansen²⁹, T. Chujo¹¹⁴, S.U. Chung⁸⁴, C. Cicalo⁹⁶, L. Cifarelli^{19,30,10}, F. Cindolo⁹⁷, J. Cleymans⁷⁹, F. Coccetti¹⁰, F. Colamaria²⁸, D. Colella²⁸, G. Conesa Balbastre⁶⁴, Z. Conesa del Valle³⁰, P. Constantin⁸², G. Contin²¹, J.G. Contreras⁹, T.M. Cormier¹¹⁹, Y. Corrales Morales²³, P. Cortese²⁷, I. Cortés Maldonado¹, M.R. Cosentino⁶⁷, F. Costa³⁰, M.E. Cotallo⁸, E. Crescio⁹, P. Crochet⁶³, E. Cruz Alaniz⁵⁶, E. Cuautle⁵⁵, L. Cunqueiro⁶⁵, A. Dainese^{20,93}, H.H. Dalsgaard⁷¹, A. Danu⁵⁰, D. Das⁸⁹, I. Das⁴², K. Das⁸⁹, A. Dash¹⁰⁸, S. Dash⁴⁰, S. De¹¹⁶, G.O.V. de Barros¹⁰⁷, A. De Caro^{26,10}, G. de Cataldo⁹⁸, J. de Cuveland³⁶, A. De Falco²², D. De Gruttola²⁶, H. Delagrangé¹⁰², A. Deloff¹⁰⁰, V. Demanov⁸⁷, N. De Marco⁹⁴, E. Dénes⁶⁰, S. De Pasquale²⁶, A. Deppman¹⁰⁷, G. D'Erasmus²⁸, R. de Rooij⁴⁵, M.A. Diaz Corchero⁸, D. Di Bari²⁸, T. Dietel⁵⁴, C. Di Giglio²⁸, S. Di Liberto⁹⁵, A. Di Mauro³⁰, P. Di Nezza⁶⁵, R. Divià³⁰, Ø. Djuvsland¹⁵, A. Dobrin^{119,29}, T. Dobrowolski¹⁰⁰, I. Domínguez⁵⁵, B. Dönigus⁸⁵, O. Dordic¹⁸, O. Driga¹⁰², A.K. Dubey¹¹⁶, A. Dubla⁴⁵, L. Ducroux¹⁰⁹, P. Dupieux⁶³, M.R. Dutta Majumdar¹¹⁶, A.K. Dutta Majumdar⁸⁹, D. Elia⁹⁸, D. Emschermann⁵⁴, H. Engel⁵¹, B. Erazmus^{30,102}, H.A. Erdal³², B. Espagnon⁴², M. Estienne¹⁰², S. Esumi¹¹⁴, D. Evans⁹⁰, G. Eyyubova¹⁸, D. Fabris^{20,93}, J. Faivre⁶⁴, D. Falchieri¹⁹, A. Fantoni⁶⁵, M. Fasel⁸⁵, R. Fearick⁷⁹, A. Fedunov⁵⁹, D. Fehler¹⁵, L. Feldkamp⁵⁴, D. Felea⁵⁰, B. Fenton-Olsen⁶⁷, G. Feofilov¹¹⁷, A. Fernández Téllez¹, A. Ferretti²³, R. Ferretti²⁷, A. Festanti²⁰, J. Figiel¹⁰⁴, M.A.S. Figueredo¹⁰⁷, S. Filchagin⁸⁷, D. Finogeev⁴⁴, F.M. Fionda²⁸, E.M. Fiore²⁸, M. Floris³⁰, S. Foertsch⁷⁹, P. Foka⁸⁵, S. Fokin⁸⁸, E. Fragiaco⁹², A. Francescon^{30,20}, U. Frankenfeld⁸⁵, U. Fuchs³⁰, C. Furget⁶⁴, M. Fusco Girard²⁶, J.J. Gaardhøje⁷¹, M. Gagliardi²³, A. Gago⁹¹, M. Gallio²³, D.R. Gangadharan¹⁶, P. Ganoti⁷⁴, C. Garabatos⁸⁵, E. Garcia-Solis¹¹, I. Garishvili⁶⁸, J. Gerhard³⁶, M. Germain¹⁰², C. Geuna¹², A. Gheata³⁰, M. Gheata^{50,30}, B. Ghidini²⁸, P. Ghosh¹¹⁶, P. Gianotti⁶⁵, M.R. Girard¹¹⁸, P. Giubellino³⁰, E. Gladysz-Dziadus¹⁰⁴, P. Glässel⁸², R. Gomez^{106,9}, E.G. Ferreira¹³, L.H. González-Trueba⁵⁶, P. González-Zamora⁸, S. Gorbunov³⁶, A. Goswami⁸¹, S. Gotovac¹⁰³, V. Grabski⁵⁶, L.K. Graczykowski¹¹⁸, R. Grajcarek⁸², A. Grelli⁴⁵, C. Grigoras³⁰, A. Grigoras³⁰, V. Grigoriev⁶⁹, A. Grigoryan¹²¹, S. Grigoryan⁵⁹, B. Grinyov², N. Grion⁹², P. Gros²⁹, J.F. Grosse-Oetringhaus³⁰, J.-Y. Grossiord¹⁰⁹, R. Grosso³⁰, F. Guber⁴⁴, R. Guernane⁶⁴, C. Guerra Gutierrez⁹¹, B. Guerzoni¹⁹, M. Guilbaud¹⁰⁹, K. Gulbrandsen⁷¹, T. Gunji¹¹³, A. Gupta⁸⁰, R. Gupta⁸⁰, H. Gutbrod⁸⁵, Ø. Haaland¹⁵, C. Hadjidakis⁴², M. Haiduc⁵⁰, H. Hamagaki¹¹³, G. Hamar⁶⁰, B.H. Han¹⁷, L.D. Hanratty⁹⁰, A. Hansen⁷¹, Z. Harmanová-Tóthová³⁵, J.W. Harris¹²⁰, M. Hartig⁵², D. Hasegan⁵⁰, D. Hatzifotiadou⁹⁷, A. Hayrapetyan^{30,121}, S.T. Heckel⁵², M. Heide⁵⁴, H. Helstrup³², A. Herghelegiu⁷⁰, G. Herrera Corral⁹, N. Herrmann⁸², B.A. Hess¹¹⁵, K.F. Hetland³², B. Hicks¹²⁰, P.T. Hille¹²⁰, B. Hippolyte⁵⁸, T. Horaguchi¹¹⁴, Y. Hori¹¹³, P. Hristov³⁰, I. Hřivnáčová⁴²,

M. Huang¹⁵, T.J. Humanic¹⁶, D.S. Hwang¹⁷, R. Ichou⁶³, R. Ilkaev⁸⁷, I. Ilkiv¹⁰⁰, M. Inaba¹¹⁴, E. Incani²², P.G. Innocenti³⁰, G.M. Innocenti²³, M. Ippolitov⁸⁸, M. Irfan¹⁴, C. Ivan⁸⁵, V. Ivanov⁷⁵, A. Ivanov¹¹⁷, M. Ivanov⁸⁵, O. Ivanytskyi², P. M. Jacobs⁶⁷, H.J. Jang⁶², M.A. Janik¹¹⁸, R. Janik³³, P.H.S.Y. Jayarathna¹¹⁰, S. Jena⁴⁰, D.M. Jha¹¹⁹, R.T. Jimenez Bustamante⁵⁵, L. Jirde³⁰, P.G. Jones⁹⁰, H. Jung³⁷, A. Jusko⁹⁰, A.B. Kaidalov⁴⁶, V. Kakoyan¹²¹, S. Kalcher³⁶, P. Kaliňák⁴⁷, T. Kalliokoski³⁸, A. Kalweit^{53,30}, J.H. Kang¹²³, V. Kaplin⁶⁹, A. Karasu Uysal^{30,122}, O. Karavichev⁴⁴, T. Karavicheva⁴⁴, E. Karpechev⁴⁴, A. Kazantsev⁸⁸, U. Kebschull⁵¹, R. Keidel¹²⁴, M.M. Khan¹⁴, S.A. Khan¹¹⁶, P. Khan⁸⁹, A. Khanzadeev⁷⁵, Y. Kharlov⁴³, B. Kileng³², M. Kim¹²³, D.W. Kim³⁷, J.H. Kim¹⁷, J.S. Kim³⁷, M. Kim³⁷, S. Kim¹⁷, D.J. Kim³⁸, B. Kim¹²³, T. Kim¹²³, S. Kirsch³⁶, I. Kisel³⁶, S. Kiselev⁴⁶, A. Kisiel¹¹⁸, J.L. Klay⁴, J. Klein⁸², C. Klein-Bösing⁵⁴, M. Kliemant⁵², A. Kluge³⁰, M.L. Knichel⁸⁵, A.G. Knospe¹⁰⁵, K. Koch⁸², M.K. Köhler⁸⁵, T. Kollegger³⁶, A. Kolojvari¹¹⁷, V. Kondratiev¹¹⁷, N. Kondratyeva⁶⁹, A. Konevskikh⁴⁴, A. Korneev⁸⁷, R. Kour⁹⁰, M. Kowalski¹⁰⁴, S. Kox⁶⁴, G. Koyithatta Meethalevedu⁴⁰, J. Kral³⁸, I. Králik⁴⁷, F. Kramer⁵², I. Kraus⁸⁵, T. Krawutschke^{82,31}, M. Krelina³⁴, M. Kretz³⁶, M. Krivda^{90,47}, F. Krizek³⁸, M. Krus³⁴, E. Kryshen⁷⁵, M. Krzewicki⁸⁵, Y. Kucheriaev⁸⁸, T. Kugathasan³⁰, C. Kuhn⁵⁸, P.G. Kuijter⁷², I. Kulakov⁵², J. Kumar⁴⁰, P. Kurashvili¹⁰⁰, A. Kurepin⁴⁴, A.B. Kurepin⁴⁴, A. Kuryakin⁸⁷, S. Kuschpil⁷³, V. Kuschpil⁷³, H. Kvaerno¹⁸, M.J. Kweon⁸², Y. Kwon¹²³, P. Ladrón de Guevara⁵⁵, I. Lakomov⁴², R. Langoy¹⁵, S.L. La Pointe⁴⁵, C. Lara⁵¹, A. Lardeux¹⁰², P. La Rocca²⁵, R. Lea²¹, Y. Le Bornec⁴², M. Lechman³⁰, K.S. Lee³⁷, S.C. Lee³⁷, G.R. Lee⁹⁰, F. Lefèvre¹⁰², J. Lehnert⁵², M. Lenhardt⁸⁵, V. Lenti⁹⁸, H. León⁵⁶, M. Leoncino⁹⁴, I. León Monzón¹⁰⁶, H. León Vargas⁵², P. Lévai⁶⁰, J. Lien¹⁵, R. Lietava⁹⁰, S. Lindal¹⁸, V. Lindenstruth³⁶, C. Lippmann^{85,30}, M.A. Lisa¹⁶, L. Liu¹⁵, V.R. Loggins¹¹⁹, V. Loginov⁶⁹, S. Lohn³⁰, D. Lohner⁸², C. Loizides⁶⁷, K.K. Loo³⁸, X. Lopez⁶³, E. López Torres⁷, G. Løvholden¹⁸, X.-G. Lu⁸², P. Luettig⁵², M. Lunardon²⁰, J. Luo⁵, G. Luparello⁴⁵, L. Luquin¹⁰², C. Luzzi³⁰, R. Ma¹²⁰, K. Ma⁵, D.M. Madagodahettige-Don¹¹⁰, A. Maevskaya⁴⁴, M. Mager^{53,30}, D.P. Mahapatra⁴⁸, A. Maire⁸², M. Malaev⁷⁵, I. Maldonado Cervantes⁵⁵, L. Malinina^{59,ii}, D. Mal'Kevich⁴⁶, P. Malzacher⁸⁵, A. Mamonov⁸⁷, L. Mangotra⁸⁰, V. Manko⁸⁸, F. Manso⁶³, V. Manzari⁹⁸, Y. Mao⁵, M. Marchisone^{63,23}, J. Mareš⁴⁹, G.V. Margagliotti^{21,92}, A. Margotti⁹⁷, A. Marín⁸⁵, C.A. Marin Tobon³⁰, C. Markert¹⁰⁵, I. Martashvili¹¹², P. Martinengo³⁰, M.I. Martínez¹, A. Martínez Davalos⁵⁶, G. Martínez García¹⁰², Y. Martynov², A. Mas¹⁰², S. Masciocchi⁸⁵, M. Masera²³, A. Masoni⁹⁶, L. Massacrier¹⁰², A. Mastroserio²⁸, Z.L. Matthews⁹⁰, A. Matyjka^{104,102}, C. Mayer¹⁰⁴, J. Mazer¹¹², M.A. Mazzoni⁹⁵, F. Meddi²⁴, A. Menchaca-Rocha⁵⁶, J. Mercado Pérez⁸², M. Meres³³, Y. Miake¹¹⁴, L. Milano²³, J. Milosevic^{18,ii}, A. Mischke⁴⁵, A.N. Mishra⁸¹, D. Miśkowiec^{85,30}, C. Mitu⁵⁰, J. Mlynarz¹¹⁹, B. Mohanty¹¹⁶, L. Molnar^{60,30}, L. Montaño Zetina⁹, M. Monteno⁹⁴, E. Montes⁸, T. Moon¹²³, M. Morando²⁰, D.A. Moreira De Godoy¹⁰⁷, S. Moretto²⁰, A. Morsch³⁰, V. Muccifora⁶⁵, E. Mudnic¹⁰³, S. Muhuri¹¹⁶, M. Mukherjee¹¹⁶, H. Müller³⁰, M.G. Munhoz¹⁰⁷, L. Musa³⁰, A. Musso⁹⁴, B.K. Nandi⁴⁰, R. Nania⁹⁷, E. Nappi⁹⁸, C. Nattrass¹¹², N.P. Naumov⁸⁷, S. Navin⁹⁰, T.K. Nayak¹¹⁶, S. Nazarenko⁸⁷, G. Nazarov⁸⁷, A. Nedosekin⁴⁶, M. Nicassio²⁸, M. Niclescu^{50,30}, B.S. Nielsen⁷¹, T. Niida¹¹⁴, S. Nikolaev⁸⁸, V. Nikolic⁸⁶, S. Nikulin⁸⁸, V. Nikulin⁷⁵, B.S. Nilsen⁷⁶, M.S. Nilsson¹⁸, F. Noferini^{97,10}, P. Nomokonov⁵⁹, G. Nooren⁴⁵, N. Novitzky³⁸, A. Nyman⁸⁸, A. Nyatha⁴⁰, C. Nygaard⁷¹, J. Nystrand¹⁵, A. Ochirov¹¹⁷, H. Oeschler^{53,30}, S. Oh¹²⁰, S.K. Oh³⁷, J. Oleniacz¹¹⁸, C. Oppedisano⁹⁴, A. Ortiz Velasquez^{29,55}, G. Ortona²³, A. Oskarsson²⁹, P. Ostrowski¹¹⁸, J. Otwinowski⁸⁵, K. Oyama⁸², K. Ozawa¹¹³, Y. Pachmayer⁸², M. Pachr³⁴, F. Padilla²³, P. Pagano²⁶, G. Paic⁵⁵, F. Painke³⁶, C. Pajares¹³, S.K. Pal¹¹⁶, A. Palaha⁹⁰, A. Palmeri⁹⁹, V. Papikyan¹²¹, G.S. Pappalardo⁹⁹, W.J. Park⁸⁵, A. Passfeld⁵⁴, B. Pastirčák⁴⁷, D.I. Patalakha⁴³, V. Paticchio⁹⁸, A. Pavlinov¹¹⁹, T. Pawlak¹¹⁸, T. Peitzmann⁴⁵, H. Pereira Da Costa¹², E. Pereira De Oliveira Filho¹⁰⁷, D. Peresunko⁸⁸, C.E. Pérez Lara⁷², E. Perez Lezama⁵⁵, D. Perini³⁰, D. Perrino²⁸, W. Peryt¹¹⁸, A. Pesci⁹⁷, V. Peskov^{30,55}, Y. Pestov³, V. Petráček³⁴, M. Petran³⁴, M. Petris⁷⁰, P. Petrov⁹⁰, M. Petrovici⁷⁰, C. Petta²⁵, S. Piano⁹², A. Piccotti⁹⁴, M. Pikna³³, P. Pillot¹⁰², O. Pinazza³⁰, L. Pinsky¹¹⁰, N. Pitz⁵², D.B. Piyarathna¹¹⁰, M. Planinic⁸⁶, M. Płoskoń⁶⁷, J. Pluta¹¹⁸, T. Pochepstov⁵⁹, S. Pochybova⁶⁰, P.L.M. Podesta-Lerma¹⁰⁶, M.G. Poghosyan^{30,23}, K. Polák⁴⁹, B. Polichtchouk⁴³, A. Pop⁷⁰, S. Porteboeuf-Houssais⁶³, V. Pospíšil³⁴, B. Potukuchi⁸⁰, S.K. Prasad¹¹⁹, R. Preghenella^{97,10}, F. Prino⁹⁴, C.A. Pruneau¹¹⁹, I. Pshenichnov⁴⁴, S. Puchagin⁸⁷, G. Puudu²², A. Pulvirenti²⁵, V. Punin⁸⁷, M. Putis³⁵, J. Putschke^{119,120}, E. Quercigh³⁰, H. Qvigstad¹⁸, A. Rachevski⁹², A. Rademakers³⁰, T.S. Rähä³⁸, J. Rak³⁸, A. Rakotozafindrabe¹², L. Ramello²⁷, A. Ramírez Reyes⁹, R. Raniwala⁸¹, S. Raniwala⁸¹, S.S. Räsänen³⁸, B.T. Rascanu⁵², D. Rathee⁷⁷, K.F. Read¹¹², J.S. Real⁶⁴, K. Redlich^{100,57}, P. Reichelt⁵², M. Reicher⁴⁵, R. Renfordt⁵², A.R. Reolon⁶⁵, A. Reshetin⁴⁴, F. Rettig³⁶, J.-P. Revol³⁰, K. Reygers⁸², L. Riccati⁹⁴, R.A. Ricci⁶⁶, T. Richert²⁹, M. Richter¹⁸, P. Riedler³⁰, W. Riegler³⁰, F. Riggi^{25,99}, B. Rodrigues Fernandes Rabacal³⁰, M. Rodríguez Cahuantzi¹, A. Rodríguez Manso⁷², K. Røed¹⁵, D. Rohr³⁶, D. Röhrich¹⁵, R. Romita⁸⁵, F. Ronchetti⁶⁵, P. Rosnet⁶³, S. Rossegger³⁰, A. Rossi^{30,20}, C. Roy⁵⁸, P. Roy⁸⁹, A.J. Rubio Montero⁸, R. Rui²¹,

R. Russo²³, E. Ryabinkin⁸⁸, A. Rybicki¹⁰⁴, S. Sadovsky⁴³, K. Šafařík³⁰, R. Sahoo⁴¹, P.K. Sahu⁴⁸, J. Saini¹¹⁶, H. Sakaguchi³⁹, S. Sakai⁶⁷, D. Sakata¹¹⁴, C.A. Salgado¹³, J. Salzwedel¹⁶, S. Sambyal⁸⁰, V. Samsonov⁷⁵, X. Sanchez Castro⁵⁸, L. Šándor⁴⁷, A. Sandoval⁵⁶, S. Sano¹¹³, M. Sano¹¹⁴, R. Santo⁵⁴, R. Santoro^{98,30,10}, J. Sarkamo³⁸, E. Scapparone⁹⁷, F. Scarlassara²⁰, R.P. Scharenberg⁸³, C. Schiaua⁷⁰, R. Schicker⁸², C. Schmidt⁸⁵, H.R. Schmidt¹¹⁵, S. Schreiner³⁰, S. Schuchmann⁵², J. Schukraft³⁰, Y. Schutz^{30,102}, K. Schwarz⁸⁵, K. Schweda^{85,82}, G. Scioli¹⁹, E. Scomparin⁹⁴, R. Scott¹¹², G. Segato²⁰, I. Selyuzhenkov⁸⁵, S. Senyukov⁵⁸, J. Seo⁸⁴, S. Serçi²², E. Serradilla^{8,56}, A. Sevcenco⁵⁰, A. Shabetai¹⁰², G. Shabratova⁵⁹, R. Shahoyan³⁰, S. Sharma⁸⁰, N. Sharma⁷⁷, S. Rohni⁸⁰, K. Shigaki³⁹, M. Shimomura¹¹⁴, K. Shtejer⁷, Y. Sibiriak⁸⁸, M. Siciliano²³, E. Sicking³⁰, S. Siddhanta⁹⁶, T. Siemiarczuk¹⁰⁰, D. Silvermyr⁷⁴, C. Silvestre⁶⁴, G. Simatovic^{55,86}, G. Simonetti³⁰, R. Singaraju¹¹⁶, R. Singh⁸⁰, S. Singha¹¹⁶, V. Singhal¹¹⁶, B.C. Sinha¹¹⁶, T. Sinha⁸⁹, B. Sitar³³, M. Sitta²⁷, T.B. Skaali¹⁸, K. Skjerdal¹⁵, R. Smakal³⁴, N. Smirnov¹²⁰, R.J.M. Snellings⁴⁵, C. Sjøgaard⁷¹, R. Soltz⁶⁸, H. Son¹⁷, J. Song⁸⁴, M. Song¹²³, C. Soos³⁰, F. Soramel²⁰, I. Sputowska¹⁰⁴, M. Spyropoulou-Stassinaki⁷⁸, B.K. Srivastava⁸³, J. Stachel⁸², I. Stan⁵⁰, I. Stan⁵⁰, G. Stefanek¹⁰⁰, M. Steinpreis¹⁶, E. Stenlund²⁹, G. Steyn⁷⁹, J.H. Stiller⁸², D. Stocco¹⁰², M. Stolpovskiy⁴³, K. Strabykin⁸⁷, P. Strmen³³, A.A.P. Suaide¹⁰⁷, M.A. Subieta Vásquez²³, T. Sugitate³⁹, C. Suire⁴², M. Sukhorukov⁸⁷, R. Sultanov⁴⁶, M. Šumbera⁷³, T. Susa⁸⁶, T.J.M. Symons⁶⁷, A. Szanto de Toledo¹⁰⁷, I. Szarka³³, A. Szczepankiewicz^{104,30}, A. Szostak¹⁵, M. Szymański¹¹⁸, J. Takahashi¹⁰⁸, J.D. Tapia Takaki⁴², A. Tauro³⁰, G. Tejada Muñoz¹, A. Telesca³⁰, C. Terrevoli²⁸, J. Thäder⁸⁵, D. Thomas⁴⁵, R. Tieulent¹⁰⁹, A.R. Timmins¹¹⁰, D. Tlusty³⁴, A. Toia^{36,20,93}, H. Torii¹¹³, L. Toscano⁹⁴, V. Trubnikov², D. Truesdale¹⁶, W.H. Trzaska³⁸, T. Tsuji¹¹³, A. Tumkin⁸⁷, R. Turrisi⁹³, T.S. Tveter¹⁸, J. Ulery⁵², K. Ullaland¹⁵, J. Ulrich^{61,51}, A. Uras¹⁰⁹, J. Urbán³⁵, G.M. Urciuoli⁹⁵, G.L. Usai²², M. Vajzer^{34,73}, M. Vala^{59,47}, L. Valencia Palomo⁴², S. Vallero⁸², P. Vande Vyvre³⁰, M. van Leeuwen⁴⁵, L. Vannucci⁶⁶, A. Vargas¹, R. Varma⁴⁰, M. Vasileiou⁷⁸, A. Vasiliev⁸⁸, V. Vechernin¹¹⁷, M. Veldhoen⁴⁵, M. Venaruzzo²¹, E. Vercellin²³, S. Vergara¹, R. Vernet⁶, M. Verweij⁴⁵, L. Vickovic¹⁰³, G. Viesti²⁰, O. Vikhlyantsev⁸⁷, Z. Vilakazi⁷⁹, O. Villalobos Baillie⁹⁰, Y. Vinogradov⁸⁷, L. Vinogradov¹¹⁷, A. Vinogradov⁸⁸, T. Virgili²⁶, Y.P. Viyogi¹¹⁶, A. Vodopyanov⁵⁹, K. Voloshin⁴⁶, S. Voloshin¹¹⁹, G. Volpe^{28,30}, B. von Haller³⁰, D. Vranic⁸⁵, G. Øvrebek¹⁵, J. Vrláková³⁵, B. Vulpescu⁶³, A. Vyushin⁸⁷, V. Wagner³⁴, B. Wagner¹⁵, R. Wan⁵, D. Wang⁵, M. Wang⁵, Y. Wang⁵, Y. Wang⁸², K. Watanabe¹¹⁴, M. Weber¹¹⁰, J.P. Wessels^{30,54}, U. Westerhoff⁵⁴, J. Wiechula¹¹⁵, J. Wikne¹⁸, M. Wilde⁵⁴, A. Wilk⁵⁴, G. Wilk¹⁰⁰, M.C.S. Williams⁹⁷, B. Windelband⁸², L. Xaplanteris Karampatos¹⁰⁵, C.G. Yaldo¹¹⁹, Y. Yamaguchi¹¹³, S. Yang¹⁵, H. Yang¹², S. Yasnopolskiy⁸⁸, J. Yi⁸⁴, Z. Yin⁵, I.-K. Yoo⁸⁴, J. Yoon¹²³, W. Yu⁵², X. Yuan⁵, I. Yushmanov⁸⁸, V. Zaccaro⁷¹, C. Zach³⁴, C. Zampolli⁹⁷, S. Zaporozhets⁵⁹, A. Zarochentsev¹¹⁷, P. Závada⁴⁹, N. Zaviyalov⁸⁷, H. Zbroszczyk¹¹⁸, P. Zelnicek⁵¹, I.S. Zgura⁵⁰, M. Zhalov⁷⁵, X. Zhang^{63,5}, H. Zhang⁵, F. Zhou⁵, Y. Zhou⁴⁵, D. Zhou⁵, J. Zhu⁵, X. Zhu⁵, J. Zhu⁵, A. Zichichi^{19,10}, A. Zimmermann⁸², G. Zinovjev², Y. Zoccarato¹⁰⁹, M. Zynovyev², M. Zyzak⁵²

Affiliation notes

- ⁱ Also at: M.V.Lomonosov Moscow State University, D.V.Skobeltzyn Institute of Nuclear Physics, Moscow, Russia
- ⁱⁱ Also at: University of Belgrade, Faculty of Physics and "Vinča" Institute of Nuclear Sciences, Belgrade, Serbia

Collaboration Institutes

- ¹ Benemérita Universidad Autónoma de Puebla, Puebla, Mexico
- ² Bogolyubov Institute for Theoretical Physics, Kiev, Ukraine
- ³ Budker Institute for Nuclear Physics, Novosibirsk, Russia
- ⁴ California Polytechnic State University, San Luis Obispo, California, United States
- ⁵ Central China Normal University, Wuhan, China
- ⁶ Centre de Calcul de l'IN2P3, Villeurbanne, France
- ⁷ Centro de Aplicaciones Tecnológicas y Desarrollo Nuclear (CEADEN), Havana, Cuba
- ⁸ Centro de Investigaciones Energéticas Medioambientales y Tecnológicas (CIEMAT), Madrid, Spain
- ⁹ Centro de Investigación y de Estudios Avanzados (CINVESTAV), Mexico City and Mérida, Mexico
- ¹⁰ Centro Fermi – Centro Studi e Ricerche e Museo Storico della Fisica "Enrico Fermi", Rome, Italy
- ¹¹ Chicago State University, Chicago, United States
- ¹² Commissariat à l'Energie Atomique, IRFU, Saclay, France

- 13 Departamento de Física de Partículas and IGFAE, Universidad de Santiago de Compostela, Santiago de Compostela, Spain
- 14 Department of Physics Aligarh Muslim University, Aligarh, India
- 15 Department of Physics and Technology, University of Bergen, Bergen, Norway
- 16 Department of Physics, Ohio State University, Columbus, Ohio, United States
- 17 Department of Physics, Sejong University, Seoul, South Korea
- 18 Department of Physics, University of Oslo, Oslo, Norway
- 19 Dipartimento di Fisica dell'Università and Sezione INFN, Bologna, Italy
- 20 Dipartimento di Fisica dell'Università and Sezione INFN, Padova, Italy
- 21 Dipartimento di Fisica dell'Università and Sezione INFN, Trieste, Italy
- 22 Dipartimento di Fisica dell'Università and Sezione INFN, Cagliari, Italy
- 23 Dipartimento di Fisica dell'Università and Sezione INFN, Turin, Italy
- 24 Dipartimento di Fisica dell'Università 'La Sapienza' and Sezione INFN, Rome, Italy
- 25 Dipartimento di Fisica e Astronomia dell'Università and Sezione INFN, Catania, Italy
- 26 Dipartimento di Fisica 'E.R. Caianiello' dell'Università and Gruppo Collegato INFN, Salerno, Italy
- 27 Dipartimento di Scienze e Innovazione Tecnologica dell'Università del Piemonte Orientale and Gruppo Collegato INFN, Alessandria, Italy
- 28 Dipartimento Interateneo di Fisica 'M. Merlin' and Sezione INFN, Bari, Italy
- 29 Division of Experimental High Energy Physics, University of Lund, Lund, Sweden
- 30 European Organization for Nuclear Research (CERN), Geneva, Switzerland
- 31 Fachhochschule Köln, Köln, Germany
- 32 Faculty of Engineering, Bergen University College, Bergen, Norway
- 33 Faculty of Mathematics, Physics and Informatics, Comenius University, Bratislava, Slovakia
- 34 Faculty of Nuclear Sciences and Physical Engineering, Czech Technical University in Prague, Prague, Czech Republic
- 35 Faculty of Science, P.J. Šafárik University, Košice, Slovakia
- 36 Frankfurt Institute for Advanced Studies, Johann Wolfgang Goethe-Universität Frankfurt, Frankfurt, Germany
- 37 Gangneung-Wonju National University, Gangneung, South Korea
- 38 Helsinki Institute of Physics (HIP) and University of Jyväskylä, Jyväskylä, Finland
- 39 Hiroshima University, Hiroshima, Japan
- 40 Indian Institute of Technology Bombay (IIT), Mumbai, India
- 41 Indian Institute of Technology Indore (IIT), Indore, India
- 42 Institut de Physique Nucléaire d'Orsay (IPNO), Université Paris-Sud, CNRS-IN2P3, Orsay, France
- 43 Institute for High Energy Physics, Protvino, Russia
- 44 Institute for Nuclear Research, Academy of Sciences, Moscow, Russia
- 45 Nikhef, National Institute for Subatomic Physics and Institute for Subatomic Physics of Utrecht University, Utrecht, Netherlands
- 46 Institute for Theoretical and Experimental Physics, Moscow, Russia
- 47 Institute of Experimental Physics, Slovak Academy of Sciences, Košice, Slovakia
- 48 Institute of Physics, Bhubaneswar, India
- 49 Institute of Physics, Academy of Sciences of the Czech Republic, Prague, Czech Republic
- 50 Institute of Space Sciences (ISS), Bucharest, Romania
- 51 Institut für Informatik, Johann Wolfgang Goethe-Universität Frankfurt, Frankfurt, Germany
- 52 Institut für Kernphysik, Johann Wolfgang Goethe-Universität Frankfurt, Frankfurt, Germany
- 53 Institut für Kernphysik, Technische Universität Darmstadt, Darmstadt, Germany
- 54 Institut für Kernphysik, Westfälische Wilhelms-Universität Münster, Münster, Germany
- 55 Instituto de Ciencias Nucleares, Universidad Nacional Autónoma de México, Mexico City, Mexico
- 56 Instituto de Física, Universidad Nacional Autónoma de México, Mexico City, Mexico
- 57 Institut of Theoretical Physics, University of Wrocław, Poland
- 58 Institut Pluridisciplinaire Hubert Curien (IPHC), Université de Strasbourg, CNRS-IN2P3, Strasbourg, France
- 59 Joint Institute for Nuclear Research (JINR), Dubna, Russia
- 60 KFKI Research Institute for Particle and Nuclear Physics, Hungarian Academy of Sciences, Budapest, Hungary
- 61 Kirchhoff-Institut für Physik, Ruprecht-Karls-Universität Heidelberg, Heidelberg, Germany

- 62 Korea Institute of Science and Technology Information, Daejeon, South Korea
- 63 Laboratoire de Physique Corpusculaire (LPC), Clermont Université, Université Blaise Pascal, CNRS-IN2P3, Clermont-Ferrand, France
- 64 Laboratoire de Physique Subatomique et de Cosmologie (LPSC), Université Joseph Fourier, CNRS-IN2P3, Institut Polytechnique de Grenoble, Grenoble, France
- 65 Laboratori Nazionali di Frascati, INFN, Frascati, Italy
- 66 Laboratori Nazionali di Legnaro, INFN, Legnaro, Italy
- 67 Lawrence Berkeley National Laboratory, Berkeley, California, United States
- 68 Lawrence Livermore National Laboratory, Livermore, California, United States
- 69 Moscow Engineering Physics Institute, Moscow, Russia
- 70 National Institute for Physics and Nuclear Engineering, Bucharest, Romania
- 71 Niels Bohr Institute, University of Copenhagen, Copenhagen, Denmark
- 72 Nikhef, National Institute for Subatomic Physics, Amsterdam, Netherlands
- 73 Nuclear Physics Institute, Academy of Sciences of the Czech Republic, Řež u Prahy, Czech Republic
- 74 Oak Ridge National Laboratory, Oak Ridge, Tennessee, United States
- 75 Petersburg Nuclear Physics Institute, Gatchina, Russia
- 76 Physics Department, Creighton University, Omaha, Nebraska, United States
- 77 Physics Department, Panjab University, Chandigarh, India
- 78 Physics Department, University of Athens, Athens, Greece
- 79 Physics Department, University of Cape Town, iThemba LABS, Cape Town, South Africa
- 80 Physics Department, University of Jammu, Jammu, India
- 81 Physics Department, University of Rajasthan, Jaipur, India
- 82 Physikalisches Institut, Ruprecht-Karls-Universität Heidelberg, Heidelberg, Germany
- 83 Purdue University, West Lafayette, Indiana, United States
- 84 Pusan National University, Pusan, South Korea
- 85 Research Division and ExtreMe Matter Institute EMMI, GSI Helmholtzzentrum für Schwerionenforschung, Darmstadt, Germany
- 86 Rudjer Bošković Institute, Zagreb, Croatia
- 87 Russian Federal Nuclear Center (VNIIEF), Sarov, Russia
- 88 Russian Research Centre Kurchatov Institute, Moscow, Russia
- 89 Saha Institute of Nuclear Physics, Kolkata, India
- 90 School of Physics and Astronomy, University of Birmingham, Birmingham, United Kingdom
- 91 Sección Física, Departamento de Ciencias, Pontificia Universidad Católica del Perú, Lima, Peru
- 92 Sezione INFN, Trieste, Italy
- 93 Sezione INFN, Padova, Italy
- 94 Sezione INFN, Turin, Italy
- 95 Sezione INFN, Rome, Italy
- 96 Sezione INFN, Cagliari, Italy
- 97 Sezione INFN, Bologna, Italy
- 98 Sezione INFN, Bari, Italy
- 99 Sezione INFN, Catania, Italy
- 100 Soltan Institute for Nuclear Studies, Warsaw, Poland
- 101 Nuclear Physics Group, STFC Daresbury Laboratory, Daresbury, United Kingdom
- 102 SUBATECH, Ecole des Mines de Nantes, Université de Nantes, CNRS-IN2P3, Nantes, France
- 103 Technical University of Split FESB, Split, Croatia
- 104 The Henryk Niewodniczanski Institute of Nuclear Physics, Polish Academy of Sciences, Cracow, Poland
- 105 The University of Texas at Austin, Physics Department, Austin, TX, United States
- 106 Universidad Autónoma de Sinaloa, Culiacán, Mexico
- 107 Universidade de São Paulo (USP), São Paulo, Brazil
- 108 Universidade Estadual de Campinas (UNICAMP), Campinas, Brazil
- 109 Université de Lyon, Université Lyon 1, CNRS-IN2P3, IPN-Lyon, Villeurbanne, France
- 110 University of Houston, Houston, Texas, United States
- 111 University of Technology and Austrian Academy of Sciences, Vienna, Austria
- 112 University of Tennessee, Knoxville, Tennessee, United States
- 113 University of Tokyo, Tokyo, Japan
- 114 University of Tsukuba, Tsukuba, Japan

-
- ¹¹⁵ Eberhard Karls Universität Tübingen, Tübingen, Germany
 - ¹¹⁶ Variable Energy Cyclotron Centre, Kolkata, India
 - ¹¹⁷ V. Fock Institute for Physics, St. Petersburg State University, St. Petersburg, Russia
 - ¹¹⁸ Warsaw University of Technology, Warsaw, Poland
 - ¹¹⁹ Wayne State University, Detroit, Michigan, United States
 - ¹²⁰ Yale University, New Haven, Connecticut, United States
 - ¹²¹ Yerevan Physics Institute, Yerevan, Armenia
 - ¹²² Yildiz Technical University, Istanbul, Turkey
 - ¹²³ Yonsei University, Seoul, South Korea
 - ¹²⁴ Zentrum für Technologietransfer und Telekommunikation (ZTT), Fachhochschule Worms, Worms, Germany